

## Stress wave propagation in composite materials

Siyuan J. Shen<sup>†</sup>, Jens C. Pfister<sup>‡</sup> and James D. Lee<sup>‡‡</sup>

*Department of Mechanical and Aerospace Engineering, The George Washington University,  
Washington, DC 20052, U.S.A.*

**Abstract.** The linear constitutive relations and the failure criteria of composite materials made of thermoviscoelastic solids are presented. The post-failure material behavior is proposed and the dynamic finite element equations are formulated. However, a nonlinear term is kept in the energy equation because it represents the effect of the second law of thermodynamics. A general purpose nonlinear three-dimensional dynamic finite element program COMPASS is upgraded and employed in this work to investigate the interdependence among stress wave propagation, stress concentration, failure progression and temperature elevation in composite materials. The consequence of truthfully incorporating the second law of thermodynamics is clearly observed: it will always cause temperature rise if there exists a dynamic mechanical process.

**Key words:** dynamic finite element analysis; second law of thermodynamics; thermo-mechanical coupling; thermoviscoelasticity; composite materials; wave propagation.

---

### 1. Introduction

Composite materials have had a long history, but they received little attention until the rise of the aerospace and automotive industries. In the latest three decades, the availability, diversity and applications of the high-modulus fiber-reinforced composites have increased significantly.

Composite materials are different from conventional materials for their high modulus, high strength, low density and also the superior mechanical properties that could be developed when they are formed into composite laminates. The use of composite materials could reduce weight by approximately 35% over the conventional materials in some cases (Kelly 1989). Corrosion resistance is another significant characteristics of composite materials, which enable them to be applied to almost every field irrespective of the existing adverse environmental conditions.

The increasing use of composites has made it necessary to investigate their material behaviors, their possible failure modes, the failure progression and the crack propagation, which are essential for optimizing the designs of structures made of these materials. Because of the heterogeneity and anisotropy of composite laminates, their failure characteristics are more complicated than that of the isotropic materials. Hence, the early studies were limited to special cases with simplifying assumptions. Only in the most recent years, the revolutionary advancement in computer science shed a light on this field. The availability of high capacity, high speed modern computers made it possible to analyze the failure process of fiber-reinforced composite structures in detail with finite

---

<sup>†</sup> Ph.D.

<sup>‡</sup> Master of Science

<sup>‡‡</sup> Professor

element technique.

A lot of research has been done on the progressive failure analysis of laminated composite structures. In one approach, the mechanics of matrix cracking and delamination are accounted for via locally averaged internal variables that account for the kinematics of microcracking, and damage progression is predicted by using phenomenological based damage evolution laws (Allen and Harris 1987, Allen *et al.* 1987, 1988, Lee *et al.* 1989). Solti, Mall and Robertson (1995) introduced a micromechanics based model for analyzing the response of unidirectional ceramic composites, which are subjected to uniaxial, quasi-static tension. The work by Voyiadjis and Kattan (1993) is also interesting. Some progressive failure analyses of laminated composites similar to the approach in this paper have been performed by Hwang and Sun (1989), Tolson and Zabaras (1991) and Pachajoa *et al.* (1994, 1995). However, dynamic finite element analyses of composite structures are rare. Besides, those works, even if they include the fully coupled thermomechanical behavior of composite materials, are based on a linearized energy equation which neglects the effect of the second law of thermodynamics.

For the investigation of failure analysis of composite structures, appropriate failure criteria are required. A number of different failure criteria have been proposed to predict the initiation and progression of damage in a laminate, such as maximum stress criterion (Lee 1982, Pryce and Smith 1993), the fracture mechanics approach which employs a critical energy release rate or stress intensity factor (Flaggs 1985), statistical failure analyses (Fukunaga *et al.* 1984) and Hashin's failure criteria (Hashin 1980).

In this paper, the linear constitutive relations and the failure criteria of anisotropic thermoviscoelastic solids are presented. The post-failure material behavior is proposed and the dynamic finite element equations are formulated. It should be emphasized that a nonlinear term is kept in the energy equation and thus incorporated in the finite element equations, simply because the effect of the second law of thermodynamics cannot be disregarded. An integrated three-dimensional nonlinear dynamic finite element program COMPASS is upgraded and employed in this work to investigate the interdependence among wave propagation, stress concentration, failure progression and temperature elevation in composite materials. COMPASS was first developed for static stress and failure analysis of composite structure (Pachajoa 1995). Then it was further developed into a dynamic code. Now it is capable of performing nonlinear dynamic finite element analysis and has taken the effect of the thermodynamic second law into account.

## 2. Constitutive relations

In this work, the structure is considered to be made of unidirectional fiber-reinforced composite materials that are assumed to be linear thermoviscoelastic solids. That means, the strains and the temperature variations involved are small so that the higher-order terms in the constitutive equations are negligible, and that the dependent constitutive variables are only functions of the infinitesimal strain tensor  $\mathbf{e}$ , deformation rate tensor  $\mathbf{d}$ , temperature  $\theta$ , temperature gradients  $\nabla\theta$  and the Lagrangian coordinates  $\mathbf{X}$  (Eringen 1989). The constitutive relations for anisotropic thermoviscoelastic materials can now be expressed as

$$\sigma_{ij} = \sigma_{ij}(\mathbf{e}, \mathbf{d}, \theta, \nabla\theta, \mathbf{X}) \quad (1)$$

$$q_i = q_i(\mathbf{e}, \mathbf{d}, \theta, \nabla\theta, \mathbf{X}) \quad (2)$$

$$\eta = \eta(\mathbf{e}, \mathbf{d}, \theta, \nabla\theta, \mathbf{X}) \quad (3)$$

$$\psi = \psi(\mathbf{e}, \mathbf{d}, \theta, \nabla\theta, \mathbf{X}) \quad (4)$$

where  $\boldsymbol{\sigma}$ ,  $\mathbf{q}$ ,  $\eta$ ,  $\psi$  are the stress tensor, heat flux, entropy density and free-energy density, respectively.

The fundamental laws of continuum mechanics can be written as (Eringen 1989):

$$\text{Conservation of Mass} \quad \dot{\rho} + \rho v_{i,i} = 0 \quad (5)$$

$$\text{Balance of Linear Momentum} \quad \rho \dot{v}_i = \sigma_{ij,j} + \rho f_i \quad (6)$$

$$\text{Balance of Moment of Momentum} \quad \sigma_{ij} = \sigma_{ji} \quad (7)$$

$$\text{Conservation of Energy} \quad \rho \dot{\varepsilon} = \sigma_{ij} d_{ij} - q_{i,i} + \rho h \quad (8)$$

$$\text{Clausius-Duhem Inequality} \quad -\rho(\dot{\psi} + \dot{\theta}\eta) + \sigma_{ij} d_{ij} - \frac{1}{\theta} q_i \theta_{,i} \geq 0 \quad (9)$$

where  $\rho$ ,  $\mathbf{v}$ ,  $\mathbf{f}$ ,  $\varepsilon$ ,  $h$  are the density, velocity vector, body force, internal energy density and heat source, respectively. Meanwhile,  $\varepsilon$ ,  $\psi$ ,  $\theta$  and  $\eta$  are related as

$$\varepsilon = \psi + \theta\eta \quad (10)$$

Substituting Eq. (1-4) into the Clausius-Duhem inequality, we get

$$-\rho \left[ \frac{\partial \psi}{\partial e_{ij}} \dot{e}_{ij} + \frac{\partial \psi}{\partial d_{ij}} \dot{d}_{ij} + \frac{\partial \psi}{\partial \theta} \dot{\theta} + \frac{\partial \psi}{\partial \theta_{,i}} \dot{\theta}_{,i} + \dot{\theta}\eta \right] + \sigma_{ij} d_{ij} - \frac{1}{\theta} q_i \theta_{,i} \geq 0 \quad (11)$$

Since in small-strain-small-temperature-variation theory,  $\dot{\mathbf{e}} \equiv \dot{\mathbf{d}}$ , inequality (11) can be written as

$$-\rho \left[ \frac{\partial \psi}{\partial e_{ij}} \dot{d}_{ij} + \frac{\partial \psi}{\partial d_{ij}} \dot{d}_{ij} + \frac{\partial \psi}{\partial \theta} \dot{\theta} + \frac{\partial \psi}{\partial \theta_{,i}} \dot{\theta}_{,i} + \dot{\theta}\eta \right] + \sigma_{ij} d_{ij} - \frac{1}{\theta} q_i \theta_{,i} \geq 0 \quad (12)$$

This inequality must be satisfied for all independent thermomechanical processes. Since  $\dot{\theta}$ ,  $\dot{\theta}_{,i}$  and  $\dot{\mathbf{d}}$  occur only linearly with coefficients which are not functions of these quantities, inequality (12) cannot be maintained for all  $\dot{\theta}$ ,  $\dot{\theta}_{,i}$  and  $\dot{\mathbf{d}}$  unless the coefficients of these terms vanish separately, i.e.

$$\eta = -\frac{\partial \psi}{\partial \theta} \quad (13)$$

$$\frac{\partial \psi}{\partial \theta_{,i}} = 0 \quad (14)$$

$$\frac{\partial \psi}{\partial d_{ij}} = 0 \quad (15)$$

Eqs. (14)-(15) imply that the free-energy density  $\psi$  is neither a function of  $\mathbf{d}$  nor  $\nabla\theta$ , which means

$$\psi = \psi(\mathbf{e}, \theta, \mathbf{X}) \quad (16)$$

The Clausius-Duhem inequality now takes the following form

$$\left(\sigma_{ij} - \rho \frac{\partial \Psi}{\partial e_{ij}}\right) d_{ij} - \frac{1}{\theta} q_{i,i} \geq 0 \quad (17)$$

We divide the stress tensor  $\boldsymbol{\sigma}$  into two parts, the elastic part and the dissipative part, as

$$\sigma_{ij}(\mathbf{e}, \mathbf{d}, \theta, \nabla \theta, \mathbf{X}) = {}_e\sigma_{ij}(\mathbf{e}, \theta, \mathbf{X}) + {}_d\sigma_{ij}(\mathbf{e}, \mathbf{d}, \theta, \nabla \theta, \mathbf{X}) \quad (18)$$

where

$${}_e\sigma_{ij}(\mathbf{e}, \theta, \mathbf{X}) \equiv \rho \frac{\partial \Psi}{\partial e_{ij}} \quad (19)$$

is the reversible or elastic part of the stress tensor, derivable from the free-energy density function  $\Psi$ , whereas  ${}_d\sigma_{ij}$  is the irreversible or dissipative part. Then the Clausius-Duhem inequality becomes

$${}_d\sigma_{ij} d_{ij} - \frac{1}{\theta} q_{i,i} \geq 0 \quad (20)$$

Introducing the Helmholtz free-energy potential function

$$\Sigma(\mathbf{e}, \theta, \mathbf{X}) \equiv \rho_0 \Psi(\mathbf{e}, \theta, \mathbf{X}) \quad (21)$$

where  $\rho_0$  is the initial value of  $\rho$ , the constitutive equations are now reduced to

$$\sigma_{ij} = \frac{\rho}{\rho_0} \frac{\partial \Sigma}{\partial e_{ij}} + {}_d\sigma_{ij} \quad (22)$$

$$q_i = q_i(\mathbf{e}, \mathbf{d}, \theta, \nabla \theta, \mathbf{X}) \quad (22)^*$$

$$\eta = -\frac{1}{\rho_0} \frac{\partial \Sigma}{\partial \theta} \quad (23)$$

$$\Psi = \frac{1}{\rho_0} \Sigma(\mathbf{e}, \theta, \mathbf{X}) \quad (24)$$

It is noticed that the internal energy  $\varepsilon$ , the entropy density  $\eta$ , and the elastic part of the stress tensor  ${}_e\sigma_{ij}$  are all derivable from the potential  $\Sigma$ .

Substituting Eq. (10, 22, 23) into Eq. (8), one may obtain

$$\rho \theta \dot{\eta} = {}_d\sigma_{ij} d_{ij} - q_{i,i} + \rho h \quad (25)$$

Let the absolute temperature  $\theta$  be divided into the sum of the reference temperature  $T_0$  and the temperature variation  $T$ , which is assumed to be small, i.e.,

$$\theta \equiv T_0 + T \quad \text{with } T_0 > 0, |T| \ll T_0, \quad (26)$$

then Eq. (25) can be written as

$$\rho(T_0 + T) \dot{\eta} \cong \rho T_0 \dot{\eta} = {}_d\sigma_{ij} d_{ij} - q_{i,i} + \rho h \quad (27)$$

Under zero initial stress condition,  $\Sigma$ ,  ${}_d\boldsymbol{\sigma}$  and  $\mathbf{q}$  can be expanded into polynomial forms as

$$\Sigma \cong \Sigma_0 - \rho_0 \eta_0 T - \frac{\rho_0 \gamma}{2 T_0} T^2 - \beta_{ij} e_{ij} T + \frac{1}{2} A_{ijkl} e_{ij} e_{kl} \quad (28)$$

$${}_d \sigma_{ij} \cong B_{ijkl} d_{kl} + J_{ijk} T_{,k} \quad (29)$$

$$q_i \cong -H_{ij} T_{,j} - G_{ijk} d_{jk} \quad (30)$$

where  $\Sigma_0$  and  $\eta_0$  are the reference Helmholtz free-energy potential and reference entropy density, respectively;  $\gamma$ ,  $\beta$ ,  $A$ ,  $B$ ,  $J$ ,  $H$  and  $G$  are the material coefficients which may be functions of the reference temperature and the Lagrangian coordinates, taking material inhomogeneity into consideration.

Substituting Eq. (28) into Eq. (19, 23), we get

$$\eta = \eta_0 + \frac{\gamma}{T_0} T + \frac{1}{\rho_0} \beta_{ij} e_{ij} \quad (31)$$

$${}_e \sigma_{ij} = \frac{\rho}{\rho_0} (-\beta_{ij} T + A_{ijkl} e_{kl}) \cong -\beta_{ij} T + A_{ijkl} e_{kl} \quad (32)$$

since in small strain theory,  $\frac{\rho}{\rho_0} = 1 - e_{kk} \cong 1$ .

Because the material under consideration is unidirectional fiber-reinforced, it has three mutually perpendicular planes of mirror symmetry, thus in its constitutive equations, all the odd order material property tensors have to vanish. Therefore, Eq. (29) and Eq. (30) can be reduced to

$${}_d \sigma_{ij} = B_{ijkl} d_{kl} \cong B_{ijkl} \dot{e}_{kl} \quad (33)$$

$$q_i = -H_{ij} T_{,j} \quad (34)$$

Substituting Eq. (31), (33) and (34) into Eq. (27), the energy equation becomes

$$\rho \gamma \dot{T} + T_0 \beta_{ij} \dot{e}_{ij} = B_{ijkl} \dot{e}_{ij} \dot{e}_{kl} + (H_{ij} T_{,j})_{,i} + \rho h \quad (35)$$

Similarly, the Clausius-Duhem inequality (20) turns into

$$B_{ijkl} \dot{e}_{ij} \dot{e}_{kl} + \frac{1}{\theta} H_{ij} T_{,i} T_{,j} \geq 0 \quad (36)$$

It should be noted that Eq. (35), which is the energy equation, still contains a nonlinear term  $\dot{e} : \mathbf{B} \dot{e}$ . Different from most other works done in this field, this term is kept throughout the whole work despite that the finite element formulation will become nonlinear and thus more difficult to solve. It is obvious from the inequality (36), the second law of thermodynamics, that both the second order tensor  $\mathbf{H}$  and the fourth order tensor  $\mathbf{B}$  are positive definite for unidirectional fiber-reinforced composite materials. For this reason it is not admissible to drop  $\dot{e} : \mathbf{B} \dot{e}$  from the energy equation, otherwise the effect of the second law of thermodynamics would be disregarded and the solutions would be erroneous and misleading.

Substituting Eq. (32, 33) into Eq. (6), we get

$$\rho \dot{v}_i = (A_{ijkl} e_{kl} + B_{ijkl} \dot{e}_{ij})_{,j} - \beta_{ij} T_{,j} + \rho f_i \quad (37)$$

and the thermo-mechanical coupling can be seen clearly in Eq. (35) and (37).

For unidirectional fiber-reinforced composites, we express the stress tensor  $\sigma$  in contracted notation and in the local  $LMN$ -coordinate system, which makes use of the axis symmetry about its fiber orientation labeled as the  $L$ -axis, i.e.

$$\sigma_i = -\beta_i T + A_{ij} e_j + B_{ij} \dot{e}_j \quad (38)$$

where

$$\sigma = [\sigma_{LL} \ \sigma_{MM} \ \sigma_{NN} \ \sigma_{MN} \ \sigma_{NL} \ \sigma_{LM}]' \quad (39)$$

$$e = [e_{LL} \ e_{MM} \ e_{NN} \ 2e_{MN} \ 2e_{NL} \ 2e_{LM}]' \quad (40)$$

$$\beta = [\beta_L \ \beta_M \ \beta_M \ 0 \ 0 \ 0]' \quad (41)$$

$$A = \begin{bmatrix} A_{11} & A_{12} & A_{12} & 0 & 0 & 0 \\ & A_{22} & A_{23} & 0 & 0 & 0 \\ & & A_{22} & 0 & 0 & 0 \\ & & & A_{44} & 0 & 0 \\ \text{symm.} & & & & A_{55} & 0 \\ & & & & & A_{55} \end{bmatrix} \quad (42)$$

with  $A_{44} = 1/2(A_{22} - A_{23})$ ; and the  $B$ -matrix has the same form as the  $A$ -matrix (Eringen 1989, Jones 1976).

In the local  $LMN$ -coordinate system, Eq. (34) can be written as

$$\begin{bmatrix} q_L \\ q_M \\ q_N \end{bmatrix} = - \begin{bmatrix} H_{LL} & 0 & 0 \\ 0 & H_{MM} & 0 \\ 0 & 0 & H_{MM} \end{bmatrix} \begin{bmatrix} T_{,L} \\ T_{,M} \\ T_{,N} \end{bmatrix} \quad (43)$$

The number of the independent material coefficients are 2 for  $\beta$  and  $H$  and 5 for  $A$  and  $B$ , which is well-known for second- and fourth-order tensors when the material has axis symmetry (Eringen 1989).

Up to now, we have derived the linear constitutive relations for thermoviscoelastic solid. For thermo-elastic material, the stress tensor and the energy equation are reduced to

$$\sigma_i = -\beta_i T + A_{ij} e_j \quad (44)$$

$$\rho \gamma \dot{T} + T_0 \beta_{ij} \dot{e}_{ij} = (H_{ij} T_{,j})_{,i} + \rho h \quad (45)$$

For visco-elastic material, they are reduced to

$$\sigma_i = -\beta_i T + A_{ij} e_j + B_{ij} \dot{e}_j \quad (46)$$

$$\rho \gamma \dot{T} + T_0 \beta_{ij} \dot{e}_{ij} = B_{ijkl} \dot{e}_{ij} \dot{e}_{kl} + \rho h \quad (47)$$

For elastic solid, we get

$$\sigma_i = -\beta_i T + A_{ij} e_j \quad (48)$$

$$\rho \gamma \dot{T} + T_0 \beta_{ij} \dot{e}_{ij} = \rho h \quad (49)$$

### 3. Failure criterion

In this work, Hashin's failure criterion is employed to determine whether failure occurs. It is a three-dimensional failure criterion for unidirectional fiber-reinforced composite material. There are four distinguishable failure modes (Hashin 1980):

(1) Tensile Fiber Mode ( $\sigma_{LL} \geq 0$ )

$$\left(\frac{\sigma_{LL}}{c_1}\right)^2 + \frac{(\sigma_{LM}^2 + \sigma_{LN}^2)}{c_6^2} = 1 \quad (50)$$

(2) Compressive Fiber Mode ( $\sigma_{LL} < 0$ )

$$\left(\frac{\sigma_{LL}}{c_2}\right)^2 = 1 \quad (51)$$

(3) Tensile Matrix Mode ( $\sigma_{MM} + \sigma_{NN} \geq 0$ )

$$\left(\frac{\sigma_{MM} + \sigma_{NN}}{c_3}\right)^2 + \frac{\sigma_{MN}^2 - \sigma_{MM}\sigma_{NN}}{c_5^2} + \frac{\sigma_{LM}^2 + \sigma_{LN}^2}{c_6^2} = 1 \quad (52)$$

(4) Compressive Matrix Mode ( $\sigma_{MM} + \sigma_{NN} < 0$ )

$$c(\sigma_{MM} + \sigma_{NN}) + \frac{(\sigma_{MM} + \sigma_{NN})^2}{4c_5^2} + \frac{\sigma_{MN}^2 - \sigma_{MM}\sigma_{NN}}{c_5^2} + \frac{\sigma_{LM}^2 + \sigma_{LN}^2}{c_6^2} = 1 \quad (53)$$

where

$$c = \frac{1}{c_4} \left[ \left(\frac{c_4}{2c_5}\right)^2 - 1 \right] \quad (54)$$

When failure occurs in an element, the material properties, namely, the matrices  $\beta$ ,  $H$ ,  $A$  and  $B$ , of that failed element will be modified accordingly to the failure mode (Pachajoa *et al.* 1994). For example, if an element suffers tensile fiber breakage, then (1)  $\sigma_{LL}$ ,  $\sigma_{LM}$ ,  $\sigma_{LN}$  and  $q_L$  are reduced to zero irrespective of the strains, the strain rates, or the temperature gradients, (2)  $e_{LL}$ ,  $e_{LM}$ ,  $e_{LN}$ ,  $\dot{e}_{LL}$ ,  $\dot{e}_{LM}$ ,  $\dot{e}_{LN}$  have no effect on the non-vanishing stress components. This implies that after the fibers of the element break, the matrices  $\beta$ ,  $H$ ,  $A$  and  $B$  take the following forms for the failed element

$$\beta = [0 \ \beta_M \ \beta_M \ 0 \ 0 \ 0]', \quad H = \begin{bmatrix} 0 & 0 & 0 \\ 0 & H_M & 0 \\ 0 & 0 & H_M \end{bmatrix}$$

$$\mathbf{A} = \begin{bmatrix} 0 & 0 & 0 & 0 & 0 & 0 \\ & A_{22} & A_{23} & 0 & 0 & 0 \\ & & A_{22} & 0 & 0 & 0 \\ & & & A_{44} & 0 & 0 \\ \text{symm.} & & & & 0 & 0 \\ & & & & & 0 \end{bmatrix}, \quad \mathbf{B} = \begin{bmatrix} 0 & 0 & 0 & 0 & 0 & 0 \\ & B_{22} & B_{23} & 0 & 0 & 0 \\ & & B_{22} & 0 & 0 & 0 \\ & & & B_{44} & 0 & 0 \\ \text{symm.} & & & & 0 & 0 \\ & & & & & 0 \end{bmatrix}$$

The modifications of these matrices for other failure modes can be found (Pachajoa *et al.* 1994, Pfister 1998).

#### 4. Finite element formulation

In this work, the finite element equations based on the principle of virtual work are formulated. Multiplying Eq. (6) by the virtual displacement  $\delta u_i$  and then integrating over the volume  $v$ , applying the Green-Gauss theorem, we obtain the virtual work equation as follow

$$\int \sigma_{ij} n_j \delta u_i ds - \int \sigma_{ij} \delta e_{ij} dv + \int \rho f_i \delta u_i dv - \int \rho v_i \delta u_i dv = 0 \quad (55)$$

where  $s$  is the bounding surface of the volume  $v$ . Similarly, from Eq. (35) we obtain

$$\int \rho \gamma \dot{T} \delta T dv + \int T_0 \beta_{ij} \dot{e}_{ij} \delta T dv - \int B_{ijkl} \dot{e}_{ij} \dot{e}_{kl} \delta T dv + \int q_i n_i \delta T ds - \int q_i \delta T_{,i} dv - \int \rho h \delta T dv = 0 \quad (56)$$

The surface integral in Eq. (55) can be reduced to

$$\int \sigma_{ij} n_j \delta u_i ds = \int_{s_\sigma} \sigma_i^* \delta u_i ds \quad (57)$$

where  $s_\sigma$  is the part of surface on which the stress vector  $\sigma_{ij} n_j$  is specified to be  $\sigma_i^*$ . The other part of the surface where the displacement vector  $\mathbf{u}$  is specified does not contribute to the integral, because  $\delta u_i$  is zero. Similarly, the surface integral in Eq. (56) can be reduced to

$$\int q_i n_i \delta T ds = \int_{s_q} q^* \delta T ds \quad (58)$$

where  $s_q$  is the part of surface on which the outward heat flux is specified to be  $q^*$ .

In finite element analysis, the displacement field and temperature field within an element can be calculated via the corresponding nodal values of that element as

$$u_i = N_{i\alpha} U_\alpha \quad (59)$$

$$T = N_\beta T_\beta \quad (60)$$

where  $N_{i\alpha}$  and  $N_\beta$  are matrices made of shape functions,  $U_\alpha$  and  $T_\beta$  are the nodal displacements and temperature variations, respectively. Then the strains and the temperature gradient are obtained as

$$e_{ij} = D_{ij\alpha} U_\alpha \quad (61)$$

$$T_{,i} = E_{i\beta} T_{\beta} \quad (62)$$

where  $D_{ij\alpha}$  and  $E_{i\beta}$  are derivable from the shape functions and the geometry of the element. Similarly, the virtual strains, the virtual temperature variation, and their time derivatives within an element follow the same pattern. Then by substituting the above expressions and Eq. (34, 38, 57, 58) into Eq. (55, 56), respectively, we obtain

$$(M_{\alpha\beta} \ddot{U}_{\alpha} + C_{\alpha\beta} \dot{U}_{\alpha} + K_{\alpha\beta} U_{\alpha} - P_{\alpha\beta} T_{\alpha} - F_{\beta}) \delta U_{\beta} = 0 \quad (63)$$

$$(G_{\alpha\beta} \dot{T}_{\alpha} + L_{\alpha\beta} T_{\alpha} + T_0 P_{\beta\alpha} \dot{U}_{\alpha} - Q_{\beta}) \delta T_{\beta} = 0 \quad (64)$$

where

$$M_{\alpha\beta} \equiv \int \rho N_{i\alpha} N_{i\beta} dv = M_{\beta\alpha} \quad (65)$$

$$C_{\alpha\beta} \equiv \int B_{ijkl} D_{ij\alpha} D_{kl\beta} dv = C_{\beta\alpha} \quad (66)$$

$$K_{\alpha\beta} \equiv \int A_{ijkl} D_{ij\alpha} D_{kl\beta} dv = K_{\beta\alpha} \quad (67)$$

$$P_{\alpha\beta} \equiv \int \beta_{ij} N_{\alpha} D_{ij\beta} dv \neq P_{\beta\alpha} \quad (68)$$

$$F_{\beta} \equiv \int_{s_{\sigma}} \sigma_i^* N_{i\beta} ds + \int \rho f_i N_{i\beta} dv \quad (69)$$

$$G_{\alpha\beta} \equiv \int \rho \gamma N_{\alpha} N_{\beta} dv = G_{\beta\alpha} \quad (70)$$

$$L_{\alpha\beta} \equiv \int H_{ij} E_{j\alpha} E_{i\beta} dv = L_{\beta\alpha} \quad (71)$$

$$Q_{\beta} \equiv \int \rho h N_{\beta} dv - \int_{s_q} q^* N_{\beta} ds + \dot{U}_{\alpha} \dot{U}_{\gamma} \int B_{ijkl} D_{ij\alpha} D_{kl\gamma} N_{\beta} dv \quad (72)$$

The virtual work Eq. (63, 64) should be valid for any arbitrary  $\delta U_{\beta}$  and  $\delta T_{\beta}$ , therefore, the following conditions must be satisfied

$$M\ddot{U} + C\dot{U} + KU - PT = F \quad (73)$$

$$GT + LT + T_0 P^T \dot{U} = Q \quad (74)$$

It can be seen from Eq. (73, 74) that the displacement field and the temperature field are coupled and the coupling is through the matrix  $P$ , which is related to  $\beta$ , the thermal expansion coefficients. It is also noticed that the non-linear term representing the effect of thermodynamic second law,  $\dot{\epsilon} : B \dot{\epsilon}$ , is included in matrix  $Q$ .

## 5. Stress wave propagation in composite laminate

The objective is to investigate the interdependence among wave propagation, stress concentration, failure progression, and temperature evaluation in fiber-reinforced composite materials. In this work, we consider a specimen with a central crack as shown in Fig. 1. The angle between the fibers and

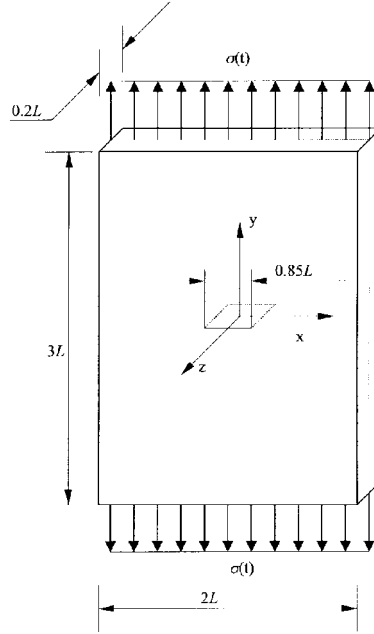


Fig. 1 Specimen with a central crack

the  $x$ -axis is  $60^\circ$ . The plate is subjected to a half-sinusoidal stress impulse  $\sigma(t)$  that acts in  $y$ -direction with the following form

$$\sigma(t) = \begin{cases} \sigma^* \sin\left(\frac{\pi t}{t_d}\right) & 0 \leq t \leq t_d \\ 0 & t > t_d \end{cases} \quad (75)$$

where  $\sigma^*$  is the amplitude of the applied stress, set to 0.3 GPa in this work;  $t_d$  is the duration of the half-sinusoidal wave.

The overall width of the specimen is  $2L$ , the height is  $3L$  and the thickness is  $0.2L$ . The length of the crack is  $0.85L$ . The specimen possesses both rotational symmetry of  $180^\circ$  about the  $z$ -axis and mirror symmetry with respect to the  $xy$  plane at  $z=0$ , therefore, only a quarter of the specimen needs to be modeled if we appropriately specify the boundary conditions as

(1) At  $y = \pm 1.5L$

$$\sigma_{yy} = \sigma(t), \quad \sigma_{yx} = \sigma_{yz} = 0 \quad (76)$$

which means there is a uniform tensile stress  $\sigma_{yy} = \sigma(t)$  being applied at these two surfaces.

(2) At  $x = L$

$$\sigma_{xx} = \sigma_{xy} = \sigma_{xz} = 0 \quad (77)$$

which means it is a stress free surface.

(3) At  $z=0.1L$

$$\sigma_{zz} = \sigma_{zx} = \sigma_{zy} = 0 \quad (78)$$

which means it is also a stress free surface.

(4) At  $x=0$

$$u_x(0, y, z, t) = -u_x(0, -y, z, t) \quad (79)$$

$$u_y(0, y, z, t) = -u_y(0, -y, z, t) \quad (80)$$

$$u_z(0, y, z, t) = u_z(0, -y, z, t) \quad (81)$$

$$T(0, y, z, t) = T(0, -y, z, t) \quad (82)$$

where  $u_x$ ,  $u_y$  and  $u_z$  are the displacements in  $x$ -,  $y$ - and  $z$ -directions, respectively.

(5) At  $z=0$

$$u_z = \sigma_{zx} = \sigma_{zy} = 0 \quad (83)$$

which means this is a plane of mirror symmetry.

(6) At  $y=0$  and  $0 \leq x \leq 0.425L$

$$\sigma_{yy} = \sigma_{yx} = \sigma_{yz} = 0 \quad (84)$$

which means that the crack surface is also a stress free surface.

It is also assumed that all the surfaces are insulated. In other words, there is only heat conduction

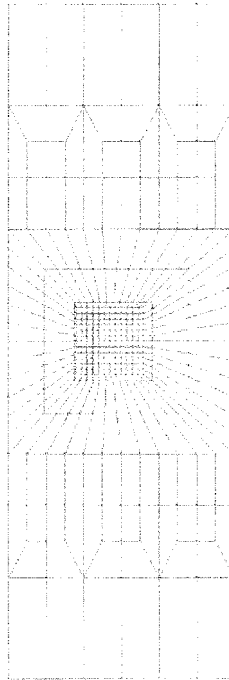


Fig. 2 Finite element mesh of the specimen

Table 1 Material properties used in the thermoviscoelastic case

Material constants	Values
Elastic modulus in fiber (L) direction	150 GPa
Elastic modulus in matrix (M) direction	7.5 GPa
Poisson's ratio in LM direction	0.25
Poisson's ratio in MN direction	0.45
Shear modulus in LM direction	6.0 GPa
Thermal expansion in fiber (L) direction	-0.03 MPa/°K
Thermal expansion in matrix (M) direction	0.6 MPa/°K
Thermal conductivity coefficient in fiber (L) direction	0.5 N/sec °K
Thermal conductivity coefficient in matrix (M) direction	0.08 N/sec °K
Damping coefficient $B_{11}$	2.5 KPa/sec
Damping coefficient $B_{22}$	7.5 KPa/sec
Damping coefficient $B_{12}$	2.5 KPa/sec
Damping coefficient $B_{23}$	3.75 KPa/sec
Damping coefficient $B_{55}$	3.75 KPa/sec
Density	$1.5 \times 10^3 \text{ kg/m}^3$
Specific heat	10 J/kg °K
Hashin's tensile strength in fiber direction	0.5 Gpa
Hashin's compressive strength in fiber direction	12.0 GPa
Hashin's tensile strength transverse fiber direction	50.0 MPa
Hashin's compressive strength in matrix direction	2.0 Gpa (absolute value)
Hashin's transverse shear strength	0.1 GPa
Hashin's axial shear strength	0.1 GPa

within the plate, but no heat convection between the plate and its environment. Then due to insulation or mirror symmetry, the heat flux on all the above-mentioned surfaces, unless otherwise the temperature is specified, are equal to zero, i.e.  $q=0$ . It is also assumed that the crack does not propagate under the applied load. Hence, the boundary conditions will not change during the entire failure progression process.

This quarter of the specimen is discretized with a finite element mesh consisting of 360 eight-node solid isoparametric elements and 808 nodes as shown in Fig. 2. The mesh is refined near the crack tip. In order to investigate the influence of the material properties, the calculations in this case are carried out for four subclasses: thermoviscoelastic, thermoelastic, viscoelastic and elastic composites. The material properties used in the thermoviscoelastic case are listed in Table 1.

From the numerical results of the thermoviscoelastic case, it can be seen that the applied stress impulse generates a stress wave in the plate (Fig. 3). When the wave approaches the centerline  $y=0$ , the existence of the crack causes a rise of the stresses. The stresses near the crack tip built up to reach the first climax. Then the stress wave moves on in an outward direction away from the crack tip. Consequently, the stresses near the crack tip decline. When the stress wave bounces back at the boundaries of the plate, it approaches the crack tip for a second time. This causes the stresses at the crack tip to increase again to the second maximum. This process continues and the stress wave keeps on moving although the magnitude of the wave declines due to the existence of the viscous damping (Pfister 1998).

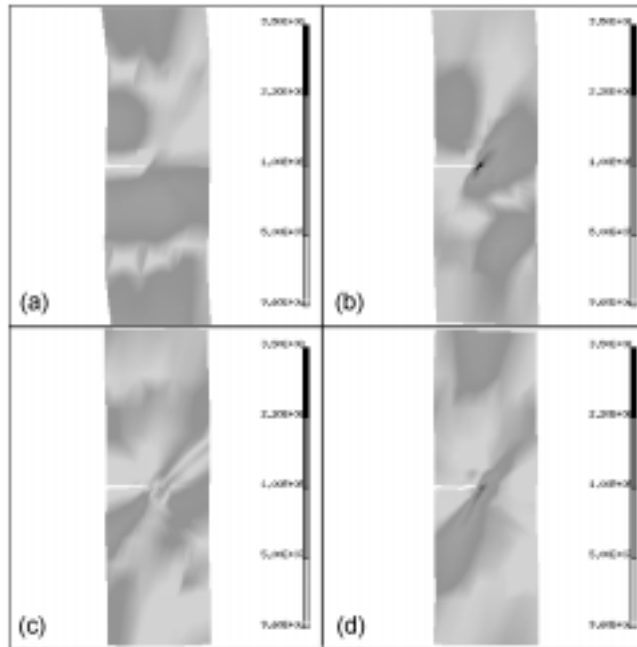


Fig. 3 Stress fields during the stress wave propagation: (a)  $t=175 \mu\text{sec}$ ; (b)  $t=225 \mu\text{sec}$ ; (c)  $t=375 \mu\text{sec}$  and (d)  $t=525 \mu\text{sec}$

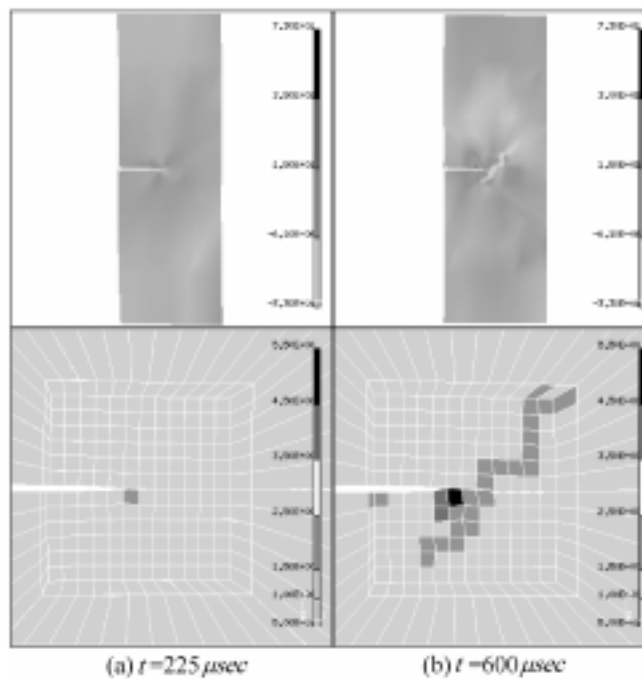


Fig. 4 Temperature fields (upper) and failure patterns (lower) during the stress wave propagation

While the stress wave bounces back and forth between the boundaries of the plate and the crack surfaces, the temperature of the whole plate increases significantly (Fig. 4). The continuous rising of temperature shows the effect of the second law of thermodynamics, which is represented by the nonlinear term  $\dot{\epsilon}:\mathbf{B}\dot{\epsilon}$  in the energy equation Eq. (35). Since we did not neglect the viscous damping of the material, the quadratic term  $\dot{\epsilon}:\mathbf{B}\dot{\epsilon}$  will always play a positive role to the temperature elevation as time goes on. Although the thermo-mechanical coupling, represented by  $\beta\dot{\epsilon}$  in the energy equation will cause the temperature to fluctuate in some local areas, the temperature rise, caused by  $\dot{\epsilon}:\mathbf{B}\dot{\epsilon}$ , in the overall field cannot be denied. This result is in accordance with the practical experience. It explains why we insist that nonlinear term must be incorporated into the finite element formulation. On the other hand, as we mentioned above, because both the influence of the thermo-mechanical coupling and the effect of the thermodynamic second law exist, the temperature distribution pattern may vary according to different material constants (Pfister 1998).

The study on failure progression shows that the first failed element appears right at the crack tip when the stress concentration is reaching its first climax (Fig. 4a). It suffers matrix failure at first, and in the end both fiber breakage and matrix failure occur (Fig. 4b). Then, according to its failure mode, its material properties are changed and hence the stresses redistribute. The high stress concentration is shifted to elements around it and this gives rise to more failures in these elements later. It can be seen that the area of failure gradually enlarges outwards. During the process of failure progression, three different kinds of failure mode appear, i.e. fiber breakage (dark grey), matrix failure (grey) and fiber breakage together with matrix failure (black). This makes the stress distribution, the temperature variation and failure progression even more complicated and variant (Fig. 3, Fig. 4).

In the analyses of the other three subclasses, the appropriate material constants are set to zero respectively. For example, in the case of thermoelastic composite, the damping coefficients are set to zero. In addition, in the cases of visco-elastic and elastic composites, we are not interested in the thermo-mechanical coupling, hence the  $\beta$ -matrix is set to zero. The results show that although the details of their stress distribution and failure progression are different from each other, they have a similar pattern as that of the thermoviscoelastic material: a stress wave is generated and moves between the boundaries and the crack surfaces; the crack tip causes stress concentration; the first failed element appears right at the crack tip when the stress concentration builds up there for the first time; the stress redistributes and brings about further failures; the failures all start from the crack tip and propagate outwards. However, the temperature fields of these three cases are quite different from each other. They are described as follow (Pfister 1998):

For thermo-elastic material, there is no damping and, as the stress wave moves between the boundaries, the temperature fluctuates up and down without any tendency. This is expected because there exists thermo-mechanical coupling however the matrix  $\mathbf{B}$  is set to zero in this case.

For visco-elastic material, it can be seen that in the beginning near the two boundaries, where the stress impulse is applied, the stress wave is generated, the temperature is high relative to that in the area where the wave has not reached. Then the temperature starts to rise significantly around the crack tip where the stress concentration occurs. While the stress wave bounces back and forth between the boundaries, the temperature keeps on increasing and the high temperature area keeps on enlarging around and in front of the crack tip. In fact, in this case the effect of the second law of thermodynamics is better recognized, since there is no thermo-mechanical coupling term, the matrix  $\mathbf{P}$  in Eq. (63, 64), to blur the picture.

For elastic material, the temperature field remains unchanged all the time, which is in our

expectation as one can see from Eq. (49) when the  $\beta$ -matrix and heat source are set to zero.

## 6. Conclusions

This work is based on a small-strain small-temperature-variation theory of thermoviscoelasticity. The constitutive relations derived are both materially and geometrically linear. However, a nonlinear term,  $\dot{\epsilon}:\mathbf{B}\dot{\epsilon}$ , is kept in the energy equation which represents the law of conservation of energy --- one of the five fundamental laws in continuum mechanics. Furthermore, the Clausius-Duhem inequality dictates that the matrix  $\mathbf{B}$  is positive definite, hence the nonlinear term  $\dot{\epsilon}:\mathbf{B}\dot{\epsilon}$  is always positive and has the effect to cause the temperature to rise. To drop this nonlinear term on the pretext of linearizing a theory is essentially equivalent to denying the effect of the second law of thermodynamics, actually the only fundamental law in continuum mechanics that is expressed in the form of an inequality, not an equation, and shows time has a sense of direction.

The finite element equations based on this theory for thermoviscoelastic solids have been formulated. First, it is noticed that the effect of the second law of thermodynamics can only be observed in dynamic processes. Therefore, in this work, the dynamic finite element analysis of stress wave propagation has been performed by utilizing the upgraded finite element program COMPASS.

Second, in the theory of thermoviscoelasticity, the effect of the second law of thermodynamics is represented only by the viscosity. Therefore, it is clearly seen that there is no temperature elevation if the theory is reduced to thermoelasticity --- the effect of viscosity is eliminated --- or to elasticity --- both viscosity and heat conduction are eliminated, although the thermo-mechanical coupling may still exist in elastic and thermoelastic solids. However, it has to be emphasized that for these materials only temperature fluctuation, not temperature elevation, may be observed because thermoelasticity and elasticity are theories describing thermodynamically reversible processes.

On the other hand, the consequence of truthfully incorporating the effect of thermodynamic second law is clearly observed as long as the material possesses viscosity: it will always cause temperature rise if there exists a dynamic mechanical process. This is the main point that the authors of this work are trying to convey.

## References

- Allen, D.H., and Harris, C.E. (1987), "A thermomechanical constitutive theory for elastic composites with distributed damage. I: Theoretical formulation", *Int. J. Solids Struct.*, **23**, 1301-1318.
- Allen, D.H., Harris, C.E., and Groves, S.E. (1987), "A thermomechanical constitutive theory for elastic composites with distributed damage. II: Application to matrix cracking in laminated composites", *Int. J. Solids Struct.*, **23**, 1319-1338.
- Allen, D.H., Harris, C.E., Groves, S.E., and Norvel, R.G. (1988), "Characteristics of stiffness loss in crossply laminates with curved matrix cracks", *J. Compos. Mater.*, **22**, 71-80.
- Eringen, A.C. (1989), *Mechanics of Continua*, Robert E. Krieger Publishing Company, Malabar, Florida.
- Flaggs, D.L. (1985), "Prediction of tensile matrix failure in composite laminates", *J. Compos. Mater.*, **19**, 29-50.
- Fukunaga, H., Chou, T.W., Peters, P.W.M., and Schulte, K. (1984), "Probabilistic failure strength analyses of graphite/epoxy cross-ply laminates", *J. Compos. Mater.*, **18**, 339-356.
- Hashin, Z. (1980), "Failure criteria for unidirectional fiber composites", *J. Appl. Mech.*, **47**, 329-334.

- Hwang, W.C., and Sun, C.T. (1989), "Failure analysis of laminated composites by using iterative three-dimensional finite element method", *Comput. and Struct.*, **33**(1), 41-47.
- Jones, R.M. (1976), *Mechanics of Composite Materials*, Technomic Publishing CO, Lancaster, PA.
- Kattan, P.I., and Voyidjis, G.Z. (1993), "Micromechanical modeling of damage in uniaxially loaded unidirectional fiber-reinforced composite laminate", *Int. J. Solids Struct.*, **30**, 19-36.
- Kelly, A. (1989), *Concise Encyclopedia of Composite Materials*, Pergamon Press, Oxford.
- Lee, J.D. (1982), "Three dimensional finite element analysis of damage accumulation in composite laminate", *Comput. and Struct.*, **15**(3), 335-350.
- Lee, J.W., Allen, D.H., and Harris, C.E. (1989), "Internal state variable approach for predicting stiffness reduction in fibrous laminated composites with matrix cracks", *J. Compos. Mater.*, **23**, 1273-1291.
- Pachajoa, M.E., Lee, K.Y., and Lee, J.D. (1994), "Progressive failure analysis of composite structures made of thermoelastic solids", *Compos. Eng.*, **4**(5), 503-523.
- Pachajoa, M.E., Frances, M.K., and Lee, J.D. (1995), "Stress and failure analysis of composite structures", *Eng. Fracture Mech.*, **50**, 883-902.
- Pfister, J. (1998), *An Integrated Three-dimensional Nonlinear Dynamic Finite Element Analysis of Wave Propagation, Stress Singularity, Failure progression, and Temperature Elevation in composite material*, Master thesis, CME department, the George Washington University.
- Pryce, A.W., and Smith, P.A. (1993), "Matrix cracking in unidirectional ceramic matrix composites under quasi-static and cyclic loading", *Acta. Metall. Mater.*, **41**(4), 1269-1281.
- Solti, J.P., Mall, S., and Robertson, D.D. (1995), "Modeling damage in unidirectional ceramic matrix composites", *Compos. Sci. and Technol.*, **54**, 55-66.
- Solti, J.P., Mall, S., and Robertson, D.D. (1995), "Modeling of progressive damage in unidirectional ceramic matrix composites", "Recent advances in composite materials", *Joint Appl. Mech. and Mater. Summer Conference*, S.R. White, H.T. Hahn and W.T. Jones, eds., Los Angeles, CA, **56**, 1-11.
- Tolson, S., and Zabbar, N. (1991), "Finite element analysis of progressive failure in laminated composite plates", *Comput. and Struct.*, **38**(3), 361-376.
- Voyidjis, G.Z., and Kattan, P.I. (1993), "Damage of fiber-reinforced composite materials with micromechanical characterization", *Int. J. Solids Struct.*, **30**, 2757-2778.